

## RESEARCH ARTICLE

# Application of sub-/supercritical fluid chromatography for the fingerprinting of a complex therapeutic peptide

Jonas Neumann<sup>1,2</sup>  | Sebastian Schmidtsdorff<sup>1,2</sup>  | Alexander H. Schmidt<sup>1</sup>  |  
Maria K. Parr<sup>2</sup> 

<sup>1</sup>Chromicent GmbH, Berlin, Germany

<sup>2</sup>Department of Biology, Chemistry, and Pharmacy, Institute of Pharmacy, Freie Universität Berlin, Berlin, Germany

## Correspondence

Jonas Neumann, Chromicent GmbH,  
Johann-Hittorf-Str. 8, 12489 Berlin,  
Germany.

Email: [jonas.neumann@chromicent.de](mailto:jonas.neumann@chromicent.de)

The application area of supercritical fluid chromatography expanded tremendously over the last years and more polar analytes such as biomolecules have become accessible. The growing interest in biopharmaceuticals and associated regulatory requirements demand alternative analytical tools. The orthogonal nature of supercritical fluid chromatography compared to reversed-phase liquid chromatography meets these needs and makes it a useful option during research and development.

In this study, we present a systematic approach for the development of a supercritical fluid chromatography method for fingerprinting of tyrothricin, a complex therapeutic peptide covering a mass range from 1200 to 1900 Da. The substance was chosen due to the presence of cyclic and linear peptides and isomeric or highly similar amino acid sequences. Different column chemistries covering neutral, basic, and zwitterionic functionalities in combination with acidic, basic, and neutral additives were screened. Subsequently, Design-of-Experiments principles were utilized to perform optimization of the chromatographic parameters. The final mass spectrometry-compatible gradient method using a diol stationary phase, carbon dioxide, and a modifier consisting of methanol/water/methanesulfonic acid (100:2:0.1, v:v:v) was found to provide orthogonality and superior resolution to other methods published. Isomeric peptide compounds coeluting in reversed-phase liquid chromatography were resolved by applying the final method.

## KEYWORDS

fingerprinting, orthogonal separation, peak capacity, supercritical fluid chromatography, therapeutic peptide

**Article Related Abbreviations:** DoE, Design-of-Experiments; MeOH, methanol; MSA, methanesulfonic acid; Rt, retention time.

This is an open access article under the terms of the [Creative Commons Attribution-NonCommercial-NoDerivs](https://creativecommons.org/licenses/by-nc-nd/4.0/) License, which permits use and distribution in any medium, provided the original work is properly cited, the use is non-commercial and no modifications or adaptations are made.

© 2022 The Authors. Journal of Separation Science published by Wiley-VCH GmbH.

## 1 | INTRODUCTION

Analytical SFC experienced a remarkable comeback over the last few years. Its application area was expanded tremendously from rather nonpolar to more polar molecules allowing the separation of a broad polarity range using a single gradient [1, 2]. Polar biomolecules (nucleotides and peptides) thus became accessible [3]. The growing interest in peptides used as therapeutics [4] comes with a growing need for analytical tools that can be used in quality control. Currently, RP-LC is the central technique in this area. Complementary knowledge about the presence of additional compounds is of primary interest, especially in the early stages of the development of pharmaceuticals. An orthogonal separation of a specific sample providing this information often is hardly achieved by applying RP-LC exclusively but can be generated by SFC [5].

Various working groups reported the use of SFC for the analysis of peptides. Cyclosporine [6], gramicidin [7–9], mixtures of chemical diverse peptides [10–13], or isomeric peptide pairs [14, 15] were used to demonstrate its potential. Even longer chain peptides up to 40 amino acids [9, 12] or larger glycoproteins up to 80 kDa were separated successfully [16, 17]. Most recently, an optimization approach of a purity method for a set of 76 linear and cyclic short-chain peptides (< 800 Da) was published. The authors utilized Derringer's desirability functions to define the overall best conditions for a single method covering all 76 peptides based on a limited number of experiments [18]. The orthogonality of RP-LC and SFC was studied subsequently for 43 of these peptides by the same group demonstrating an advantage of SFC over RP-LC due to less coelution and stronger retention. On the other hand, smaller additional peaks were detected via RP-LC [19].

In SFC, carbon dioxide is used as the major part of the eluent. Methanol (MeOH) is often added as a modifier. Water up to 7 % can be added to the modifier to increase the modifier's eluotropic strength and enhance the chromatographic performance for highly polar substances [20]. Different additives (ammonia, ammonium acetate, and others) were demonstrated to improve the separation of biomolecules [21–23]. Carbonate and hydrogen carbonate ions in the effluent were detected when a composition of water, carbon dioxide, and ammonia was used. The carbonate ions were proposed to cause a chaotropic effect enhancing the chromatographic separation of biomolecules [21]. Recently methanesulfonic acid (MSA) became a popular additive [22, 24], even if its successful usage was already reported in 1999 [13]. Its high acidity and potential to mask amino functionalities of peptides were hypothesized to enable separation of the same by SFC through synergistic effects if combined with amino derivatized stationary phases [24].

The general applicability of SFC for distinctly different peptides was proven and its beneficial use for the purification or isolation of single compounds of interest was demonstrated [23, 25]. However, very few studies have focused on methods providing sufficient selectivity to fulfill today's requirements for the application as a purity control method or the identification of a fingerprint of a complex therapeutic peptide.

With this work, we contribute to the application of SFC in peptide analysis and demonstrate its advantages. The complex peptide antibiotic tyrothricin, manufactured through fermentation processes, was chosen as an ideal model. It contains two groups of peptides: linear gramicidins and cyclic tyro- and tryptocidines (Figure 1) [26, 27]. The high number of structures possessing a high chemical similarity and covering a mass range of 1200–1900 Da made this complex of polypeptides a good candidate for this study. A systematic method development approach was applied. After defining the goals of the chromatographic method, the potential impact of the individual chromatographic parameters was ranked and investigated accordingly. Peak capacity, resolution and peak-to-valley ratio were applied as indicators for the chromatographic performance and optimized via a Design-of-Experiments (DoE) workflow. Finally, the optimized method was compared to a published RP-LC method [28], demonstrating its orthogonality and advantages.

## 2 | MATERIALS AND METHODS

### 2.1 | Chemicals and reagents

Tyrothricin chemical reference substance supplied by the European Directorate for the Quality of Medicines (Strasbourg, France) was dissolved in MeOH/water (90:10, v:v) to receive a concentration of 2 mg/ml and was used as a stock solution. MeOH and ACN (LC gradient-grade) were bought from VWR (Darmstadt, Germany). Milli-Q water was prepared freshly before use via a Merck Milli-Q system (Darmstadt, Germany) and carbon dioxide (99.995%) was derived from Air Liquide (Berlin, Germany). TFA (LC-grade,  $\geq 99.0$  %) and MSA ( $\geq 99.0$ %) were derived from Sigma Aldrich (Taufkirchen, Germany), aqueous ammonia solution (25%) and ammonium acetate (for analysis) were supplied by Merck (Darmstadt, Germany).

### 2.2 | Stationary phases

The following stationary phases were used for the SFC experiments: Torus Diol, Torus 2-PIC, Viridis BEH 2-EP from Waters (Eschborn, Germany), and a Nucleodur HILIC from Macherey-Nagel (Dinslaken, Germany). The

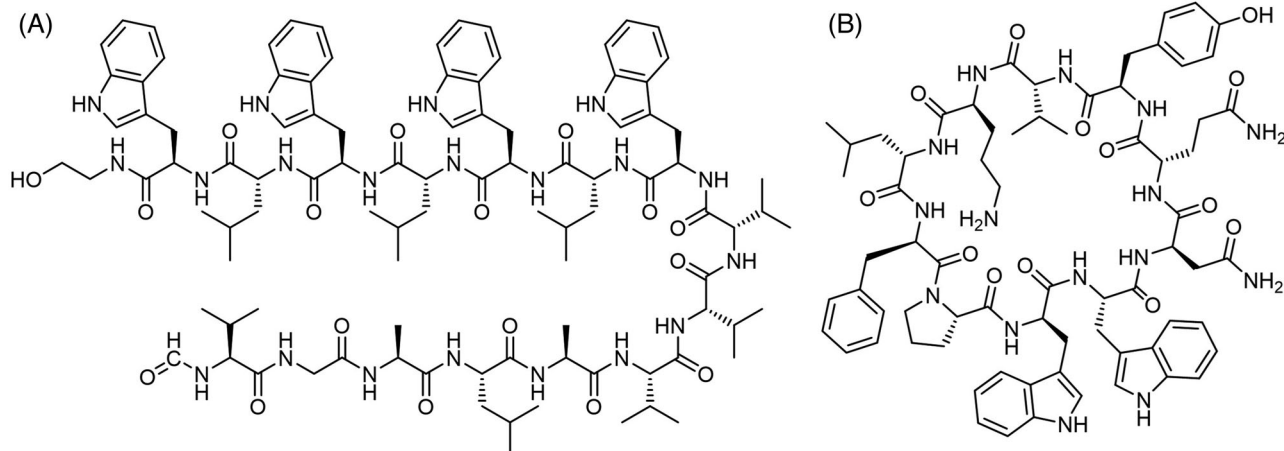


FIGURE 1 Chemical structures of the linear Val-Gramicidin A (A) and the cyclic Tyrocidine C (B) [27]

dimension of all columns was  $3.0 \times 100$  mm. The particle size was  $1.7 \mu\text{m}$  for all columns from Waters and  $1.8 \mu\text{m}$  for the HILIC column. An Acquity CSH C18 column,  $2.1 \times 100$  mm,  $1.7 \mu\text{m}$ , from Waters (Eschborn, Germany) was used for the LC experiment.

### 2.3 | Instrumentation and software

The chromatographic experiments were performed using a Waters Acquity UPC<sup>2</sup> SFC system equipped with a binary pump, a 4-port column manager with active eluent pre-heaters, an Acquity UPC<sup>2</sup> photodiode array (PDA) detector, an Acquity UPC<sup>2</sup> convergence manager (back pressure regulator) and an Acquity TQD (triple quadrupole mass spectrometer with an ESI source). A fixed-leak interface was used to connect the SFC system to the MS and a make-up solvent was provided through a Waters 515 make-up pump. An Acquity UPLC H-Class system equipped with a quaternary pump, a column manager with active eluent pre-heaters and an Acquity PDA detector hyphenated to the same Acquity TQD mass spectrometer was used for the comparison of the SFC and UHPLC method. Empower 3 was used for system control, data acquisition, and processing. Fusion QbD from S-Matrix (Eureka, USA) was used to visualize the DoE. The 2-D graphs were calculated via Microsoft Excel.

### 2.4 | Development of the SFC method

Initially, a generic gradient from 25 to 95% B in 15 min was applied at a flow rate of 0.6 ml/min using MeOH/water (100:2, v:v) as eluent B. As additives 0.1% ammonia (v:v), ammonium acetate (m:v), TFA (v:v), or MSA (v:v) were used. The column temperature was set to  $50^\circ\text{C}$  and back-

pressure to 1500 psi. Four stationary phases were screened (see Section 2.2). Tyrothricin (1 mg/ml) was injected. In the next step, the gradient time was prolonged to 25 min (25–80% B) to receive a better separation. The gradient was applied using the four columns and additives tested before. Due to inferior performance TFA was excluded. UV detection at 220 nm was used for all experiments. The number of peaks, peak width and shape and the overall separation of the compounds were used to assess the stationary phases and additives. The best combination was kept for further optimization: the diol column and eluent B consisting of MeOH/water/MSA (100:2:0.1, v:v:v).

In the first optimization experiment, the impact of the flow rate was studied and thus varied from 0.5 to 1.1 ml/min. Backpressure and column temperature were maintained. A gradient from 25 to 64% B was run in 20 min. To better compare the performance of the individual runs, a normalized sample concentration was prepared via dilution of the stock solution to study the impact of flow rate and gradient time (10, 20, and 30 min) on the peak capacity. The ratio of the analyte concentration was adjusted equivalently to the flow rate, for example, 0.5 mg/ml was injected at a flow rate of 0.5 ml/min.

In the following experiment, the flow rate was kept constant at 0.7 ml/min. The backpressure was varied from 1500 to 2500 psi, the column temperature from  $30$  to  $50^\circ\text{C}$  and the gradient time between 23 and 30 min reaching 55% B.

### 2.5 | Final SFC method

A Torus Diol column ( $2.1 \times 100$  mm,  $1.7 \mu\text{m}$ ) was used for the final method. The column temperature was set to  $41^\circ\text{C}$  and the backpressure to 1500 psi at a flow rate of 0.7 ml/min. Carbon dioxide was used as eluent A.

Eluent B (modifier) consisted of MeOH/water/MSA (100:2:0.1, v:v:v) and 1  $\mu$ l of tyrothricin (1.0 mg/ml) was injected. The following gradient profile was applied: 0–30 min: 25–55% B, 30–31 min: 55–25% B, 31–35 min: 25% B. Chromatograms were recorded at 220 nm using UV detection. A make-up (0.1 ml/min) consisting of MeOH/formic acid (100/0.1, v/v) was added for the SFC-MS experiments via the fixed leak interface. The MS was operated in positive ESI mode. The total ion chromatogram was recorded ( $m/z$  500–1500) and used for peak tracking. The following MS settings were applied: cone voltage 30 V, capillary voltage 3.0 kV, source temperature 120°C, desolvation gas temperature: 250°C and desolvation gas flow: 500 L/h.

## 2.6 | Orthogonal UHPLC method

For method comparison, a method was adapted [28]. A CSH C18 column (2.1  $\times$  100 mm, 1.7  $\mu$ m) was set to 40°C at a flow rate of 0.35 ml/min. Water/ACN/TFA (95/5/0.1, v/v/v) and water/ACN/TFA (5/95/0.1, v/v/v) were used as eluent A and B, respectively. The following gradient profile was applied: 0–10.5 min: 40–90% B, 10.5–11.9 min: 90% B, 11.9–12.6 min: 90–40% B, 12.6–16.8 min: 40% B. Chromatograms were recorded at 220 nm using UV detection. For MS detection, the parameters described in Section 2.5 were used.

## 3 | RESULTS AND DISCUSSION

### 3.1 | Definition of the method goals

In the beginning, goals were set for the future method: improvement of the resolution of the fingerprint, UV and MS compatibility, and orthogonality to existing methods [26–28].

The potential impact of the chromatographic parameters on the selectivity and thus the resolution of the fingerprint was ranked as follows: column chemistry > additive type > gradient time/end% B > column temperature > flow rate > backpressure. The parameters were studied based on this ranking. Column chemistry and potential additives were screened first.

### 3.2 | Screening of additives and column chemistry

Different stationary phases providing neutral, basic, and zwitterionic chemistries were chosen to evaluate the impact on the selectivity: diol, amino (2-EP and 2-PIC), or sulfobetaine (HILIC) derivatization. Two peak groups

(Figure 2C,D) were separated via the diol and zwitterionic derivatized stationary phase. Due to the integration of MS detection in the final step (see Section 3.3), these were identified as cyclic or linear peptides. The linear gramicidins containing alkyl or aromatic sidechains, mainly from leucine, tryptophan and valine, were eluted as the first group (retention time [Rt]: 6–8 min). The cyclic compounds containing more polar sidechains from tyrosine, asparagine or glutamine were stronger retained (Rt: > 10 min). The amino-functionalized stationary phases (Figure 2A,B) showed an inferior selectivity resulting in an elution in a smaller Rt window, which disqualified these columns for further optimization steps. Much higher retention was observed on the zwitterionic than on the diol functionality, resulting in broader peaks, which is in line with the results reported in other studies earlier for other peptides [24]. Due to the higher retention, a better resolution of the peaks of the linear group was achieved, which on the other hand, caused a worse separation of the cyclic peptides. The overall separation and the number of smaller peaks not detected on the sulfobetaine phase made the diol the better suited stationary phase.

Based on the literature summarized in the introduction, additives covering basic, neutral and acidic as well as ion-pairing characteristics were selected: ammonium acetate, TFA, ammonia, and MSA. The addition of water in a small amount was considered mandatory to improve the peak shape. An increase from 2 to 5% was also tested, but no distinct effect except slightly earlier elution and increased backpressure were observed. TFA (Figure 2A3) showed the worst performance based on the number of peaks and overall resolution detected on all columns. The other additives were comparable. Ammonium acetate (Figure 2A4) caused a baseline drift and thus was excluded. MSA (Figure 2A2) and ammonia (Figure 2A1) were comparable with MSA, resulting in a group of smaller well-separated peaks (Rt: 8.5–9.5 min) between the two groups of major peaks. Thus, MSA combined with the diol column was chosen for further optimization.

### 3.3 | Optimization of chromatographic parameters

The goal of the following experiment was to evaluate the impact of the flow rate and the gradient time. Initially, the effect on the selectivity of the column temperature was ranked higher than the flow rate. As the column temperature influences the backpressure and thus would have limited the flow rate to a smaller range if varied simultaneously, it was decided to study the temperature in the subsequent step. While a Van-Deemeter plot traditionally

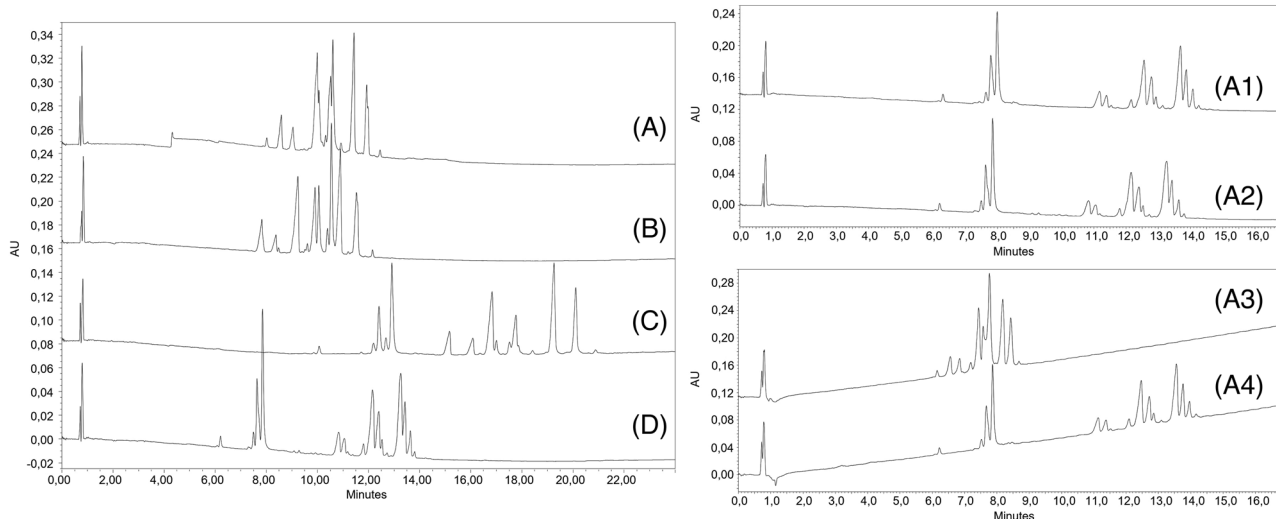


**FIGURE 2** SFC-UV chromatogram of tyrothricin separated on different stationary phases ([A] 2-PIC, [B] 2-EP, [C] HILIC, and [D] Diol) using 2% water and 0.1% methanesulfonic acid (MSA) (v/v) as the mobile phase additives in modifier methanol (MeOH). A comparison of the different additives ([A1] ammonia, [A2] MSA, [A3] TFA, and [A4] ammonium acetate) in combination with the diol column is shown

is used for the characterization of isocratic methods, the consideration of the peak capacity was demonstrated to be a viable parameter for the characterization of gradient methods [29–31]. A minimum of 0.5 ml/min was necessary to maintain sufficient pressure and thus compression of the mobile phase. An unstable baseline was observed when the flow was further reduced. A flow rate of 1.1 ml/min was estimated as the maximum based on the pressure limit of the instrument used.

Representative peaks, resolved sufficiently in all chromatograms, were chosen (Figure 3A), and the peak width of the selected peaks at 50 % height ( $W_{50\%}$ ) was calculated. The following equation, including the gradient time (tG), was used to calculate the peak capacity (P) according to Wren [32]:

$$P = 1 + \frac{tG}{1.679 \times W_{50\%}} \quad (1)$$

The factor of 1.679 was used to calculate the width at 13.4% height from the  $W_{50\%}$  peak width. This conversion was necessary to compensate for the lacking baseline separation of some peaks. The mean peak capacity was then plotted against the flow rate (Figure 3B). An increase in the mean peak capacity at higher flow rates was noted. At the same time, a logarithmic relation between the flow rate and the mean peak area was observed (Figure 3C). This effect is well known for concentration-dependent detectors such as UV [33, 34]. At a lower flow rate, the analyte remains longer in the flow cell and the response is increased. On the other hand, an increase in the detector response (either peak height

or area) results in an increased peak width. Concluding, the impact of the response on the peak width cannot be distinctly differentiated from the impact of the flow rate.

An adjustment of the sample concentration (see Section 2.4) was performed to compensate for the increasing UV response. The variation of the peak response was minimized to about 5% between the individual runs to aid comparability. As a result, the mean peak areas varied in a much smaller range, with 0.5 ml/min still giving the highest response (198 000 area and 28 000 height units) and 1.1 ml/min showing the lowest (184 000 area and 25 000 height units). This was assessed to be the more productive approach considering the goal to use peak capacity as an indicator of the performance. The optimization of the method in terms of maximizing the number of peaks and increasing their resolution, which is not impacted by a broadening of the peaks due to a higher response, was focused on. An increase in the method's sensitivity was less important at this point.

The 3-D response surface plot of the mean peak capacity (Figure 4A) shows that contrary to the observations made before, when the same sample concentration was injected for every flow rate, an increase in the peak capacity was found based on the usage of a normalized sample concentration. The lower the flow rate, the higher the mean peak capacity. The calculation of the peak capacity of peak 4 (Figure 4B) and 14 (Figure 4C), which are representative of either the first or the second group, showed converse effects of the flow rate on both peaks. A lower peak capacity caused by a broader peak was estimated for the later eluting peak. Different reasons can be hypothesized for this observation. The cyclic or linear shape and the varying

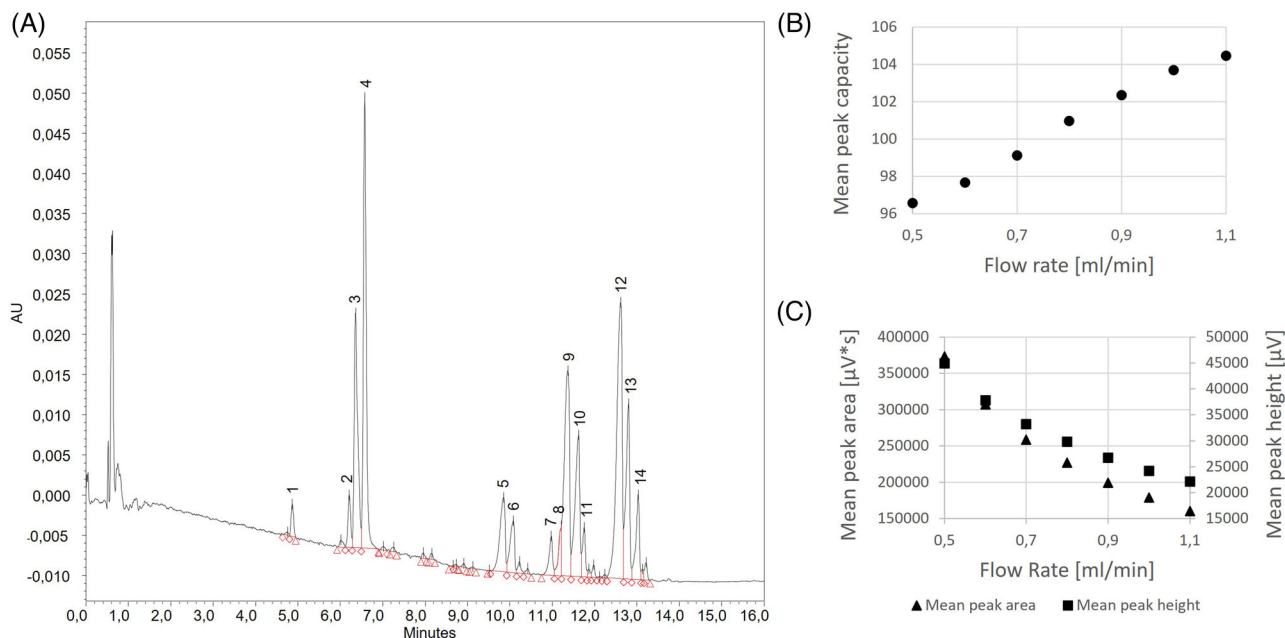


**FIGURE 3** A representative SFC-UV chromatogram is shown. The peaks 3, 4, 5, 6, 7, 9, 10, 12, and 14 provide sufficient resolution to calculate the peak width at 50% height (A). Mean peak capacity plotted against the flow rate (B). Mean peak height and area plotted against the flow rate (C)

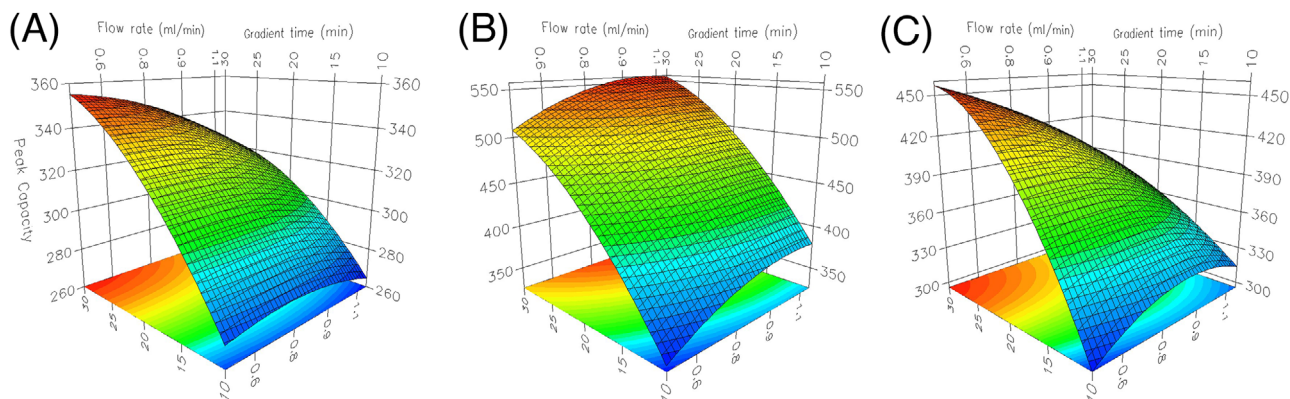


**FIGURE 4** Response surface of the peak capacity ([A] mean of representative peaks, [B] peak 4, and [C] peak 14) plotted against the flow rate and the gradient time

polarity of each component caused by the different amino acid sequences can result in other interactions with the stationary phase, which may result in varying retention characteristics. A slight fronting of the late eluting peaks can also indicate the presence of coeluting peaks. An increase in the peak width and hence a decrease in the peak capacity would then convert to an improved separation. Following this idea, a further increase in the flow rate should be beneficial to resolve these peaks. However, due to the limitation of the instrument, a further increase in the flow rate was not possible.

For the development of a purity method, a certain signal-to-noise ratio needs to be achieved for relevant impurities. Thus, a reduction of the flow rate may be considered before

increasing the sample load on the column. On the other hand, the sample load can also be reduced to increase the resolution of the peaks and maintain the signal intensity simultaneously.

Utilizing MS was also considered as an alternative to evaluating the peak width. The instrument design demands a flow split to minimize the carbon dioxide decompression before entering the MS. Adding a make-up flow prevents the analyte's precipitation and reduces the eluent's decompression. A variation of the split ratio based on the flow rate is known [35], which would add more factors affecting the analyte's response. After revisiting these factors, MS detection was discarded to evaluate peak capacity. Alternative evaporative detection

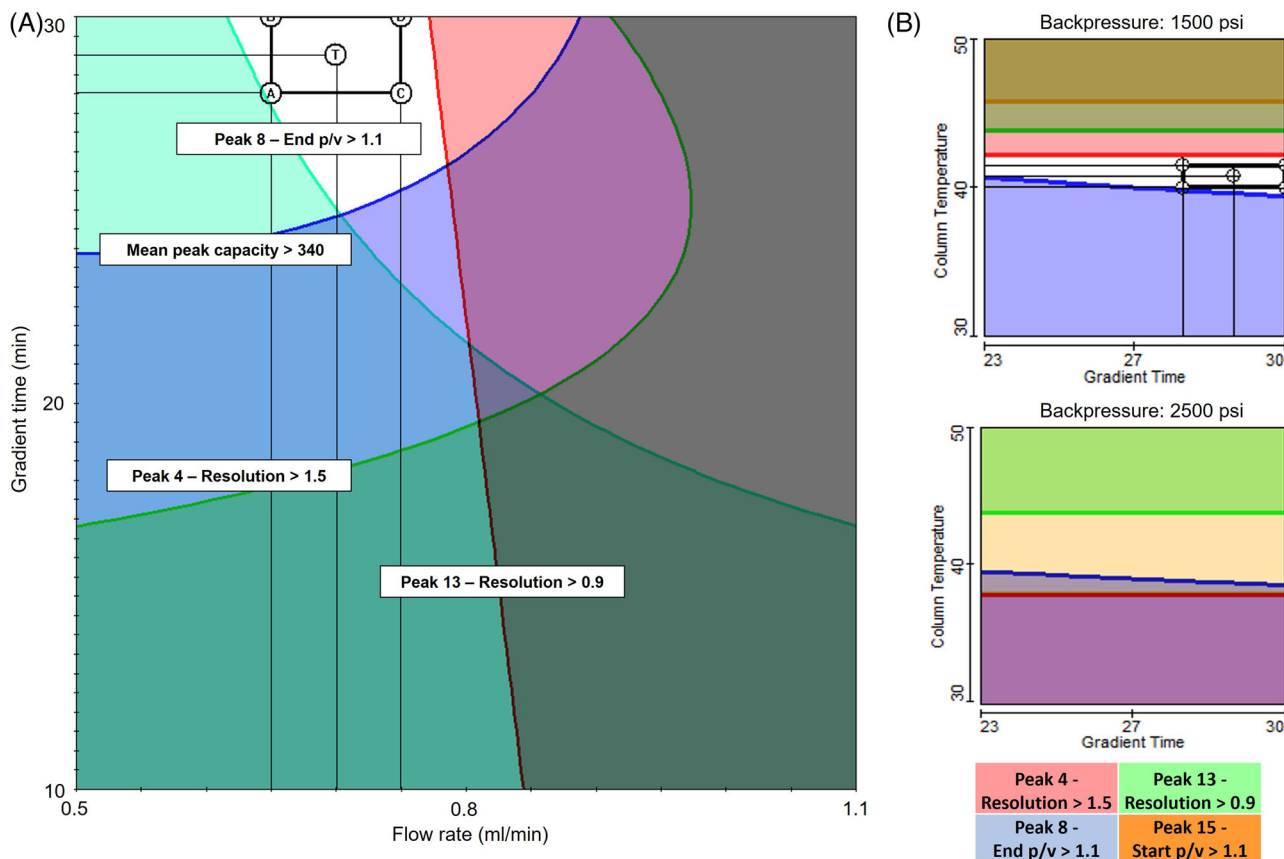


**FIGURE 5** Visualization of the impact of the chromatographic parameters gradient time and flow rate (A) and column temperature, backpressure, and gradient time (B) on the separation of critical peak pairs. Colored areas indicate conditions under which the defined goals were not achieved (note that mixed colors are possible). Therefore, white areas indicate conditions under which the best overall separation was achieved. The black box indicates conditions used for further optimization

techniques, for example, evaporative light scattering detection, also demand a split of the flow and consequently are impacted by the same factors.

However, additional performance indicators than peak capacity, which do not necessarily reflect a better resolution, then were used. Thus, the resolution between peaks 3 and 4 was chosen as an indicator for the separation of the first group and the resolution between peaks 12 and 13 for the second group. In addition, the end peak to valley ratio of peak 8 with 9 was used. Minimum values to be reached were set and maximization of these was defined as goals for the DoE (Figure 5A). For the improvement of the separation of the first group, lower rates were beneficial, but higher flow rates increased the second group's resolution. An intermediate flow rate (0.7 ml/min) was estimated as a reasonable compromise to be applicable for further optimization in combination with a prolonged gradient time.

The impact of the backpressure and the column temperature was investigated in the following experiment. The same goals as in the previous experiment were set and complemented by the peak-to-valley ratio of a newly

detectable peak. As indicated in the plot (Figure 5B), the decrease in the column temperature resulted in the separation of the additional peak 15 in the first group, which was maximized at 30°C. On the other hand, a coelution of peaks 8 and 9 is present at these conditions, which were separated at higher temperatures. An increase in the backpressure led to the coelution of peak 3 and 15, which were better separated at 1500 psi. Again, a balance between an improvement of the first and second group had to be found and 41°C combined with 1500 psi were set as the final parameters.

### 3.4 | Use as orthogonal and MS compatible technique: RP-LC versus SFC selectivity

A comparison between LC and SFC was performed to highlight the potential of using SFC as an orthogonal method. Each sample was analyzed via the newly developed SFC and the adopted LC method [28]. UV and MS

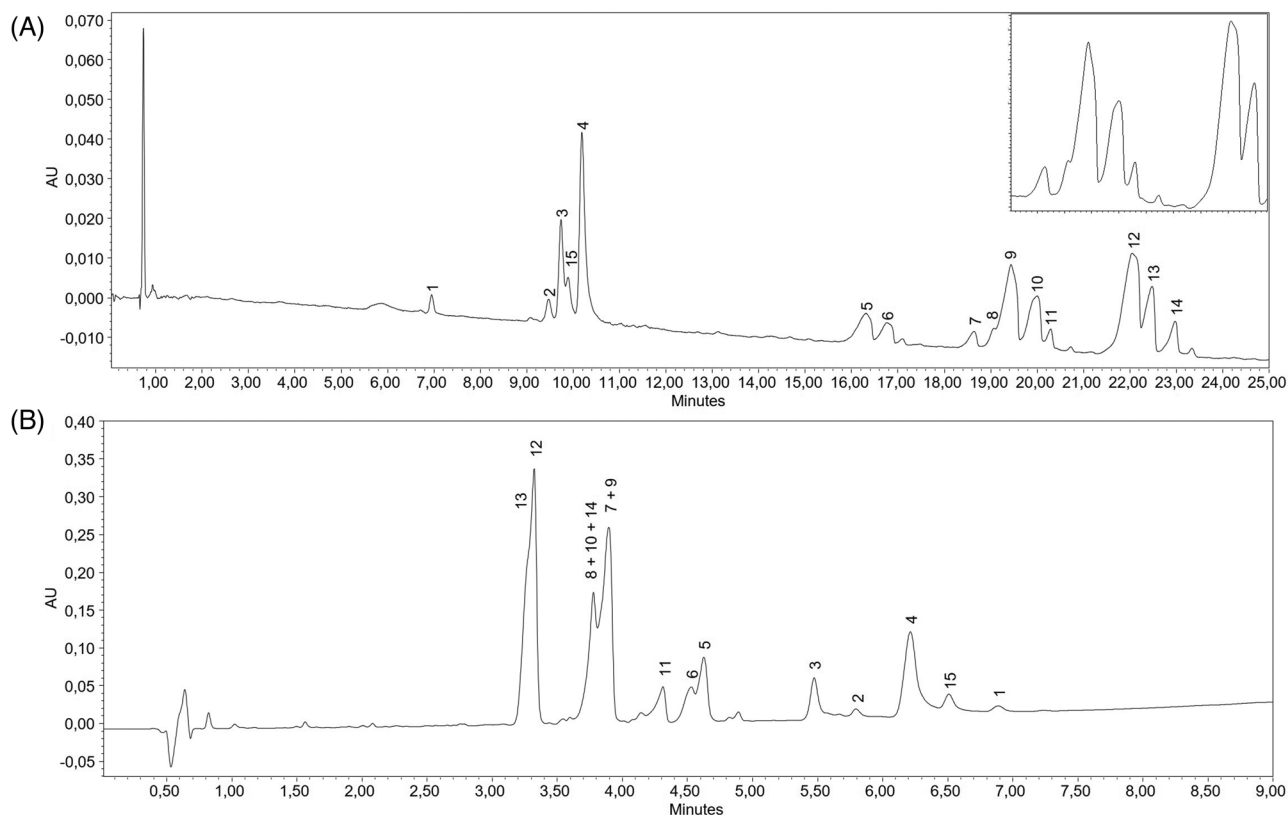


FIGURE 6 UV chromatograms of tyrothricin analyzed via the optimized SFC (A) and the adapted RP-LC method (B)

TABLE 1 Overview of the characteristic peaks detected via SFC-MS

Peak	Peptide	$m/z$ $[M+2H]^{2+}$ expected <sup>a)</sup>	$m/z$ $[M+2H]^{2+}$ detected	Rt [min]
1	Val-Gramicidin B	922.0415	922.1	6.93
2	Ile-Gramicidin C	937.0468	937.2	9.45
3	Val-Gramicidin C	930.0390	930.4	9.72
15	Ile-Gramicidin A	948.5548	948.6	9.89
4	Val-Gramicidin A	941.5470	941.9	10.17
5	Tyrocidine A	635.8351	635.9	16.30
6	Tyrocidine A1	642.8430	642.9	20.28
7/9	Tyrocidine B/B'	655.3406	655.5	18.63/19.42
8/10	Tyrocidine B1/B1'	662.3484	662.5	19.06/19.99
11	Tryptocidine B	666.8486	667.1	20.28
12	Tyrocidine C	674.8460	674.7	22.04
13	Tyrocidine C1	681.8539	682.1	22.46
14	Tryptocidine C	686.2540	686.1	22.97

<sup>a)</sup>Data obtained from Vosloo and Rautenbach [30].

detection were utilized to assign the peaks in both methods (Figure 6).

The major peaks were assigned based on the MS data published by Vosloo and Rautenbach [26]. The two peak pairs 7/9 and 8/10 (Table 1), showing the same mass signal, were detected via the SFC method. The authors describe

the presence of constitutional isomers due to a swap of tryptophan and phenylalanine at positions 3 and 4 of the amino acid sequence for tyrocidine B and B' ( $m/z$  655.5) and tyrocidine B<sub>1</sub> and B<sub>1</sub>' ( $m/z$  662.2). Concluding, separation of these isomers was achieved easily, which was not possible in other studies utilizing RP-LC [26–28].



In addition, a splitting of peaks 5, 6, 9, 10, and 12 was found using SFC. During the evaluation of the peak capacity, the presence of coeluting peaks was presumed for some peaks of the second group, which now became more evident. An increase in the overall resolution of the fingerprint was initially set as the primary goal. The optimization was consequently performed by balancing the first and second groups. Nevertheless, the observations made during the DoE-based optimization let us conclude that an increase in the flow rate may result in a better separation of these compounds if separating these individual isomers would be of main interest.

Orthogonality was achieved when comparing the elution order of the RP-LC and the SFC method. The first group is better resolved via RP-LC, but the second group can be resolved much better using SFC. This demonstrates the complementarity of both modes and the vast potential of the parallel application during research and development studies. In addition to the orthogonality, a much better overall separation of the peaks and an improvement of the overall peak shape were achieved via the SFC method. In conclusion, the goals initially defined were attained. Thus, developing a new SFC method for the fingerprinting of tyrothricin was successful.

#### 4 | CONCLUDING REMARKS

In this study, we demonstrated SFC to be superior to RP-LC for the separation of the complex peptide mixture in tyrothricin. The application of DoE principles proved to be beneficial during the optimization steps of the method to account for the contrary conditions favored by either the cyclic or the linear group. Peak capacity was shown to be an excellent indicator to rate the performance of experiments in the early steps performed during method development if complemented by others like resolution or peak-to-valley ratios. Isomeric peak pairs, which were not resolved using RP-LC, were efficiently separated. Nevertheless, RP-LC is in favor of the separation of the earlier eluting peaks, which shows that both techniques should be established in a complementary manner or that the use of SFC should be considered if separation cannot be achieved via RP-LC.

#### ACKNOWLEDGMENTS

Chromicent GmbH funded this work. We thank MACHEREY-NAGEL for the kind gift of the Nucleodur HILIC column.

#### CONFLICT OF INTEREST

The authors declare no conflict of interest.

#### AUTHOR CONTRIBUTIONS

Jonas Neumann: Conceptualization, methodology, investigation, formal analysis, visualization, and writing - original draft.

Sebastian Schmidtsdorff: Conceptualization and writing - review and editing.

Alexander H. Schmidt: Writing - review and editing and resources.


Maria K. Parr: Conceptualization, supervision, and writing - review and editing.

#### DATA AVAILABILITY STATEMENT

Data are available on request from the authors.

#### ORCID

Jonas Neumann  <https://orcid.org/0000-0001-5414-2942>

Sebastian Schmidtsdorff  <https://orcid.org/0000-0002-5881-5099>

Alexander H. Schmidt  <https://orcid.org/0000-0002-4526-7820>

Maria K. Parr  <https://orcid.org/0000-0001-7407-8300>

#### REFERENCES

1. Antonelli M, Holčapek M, Wolrab D. Ultrahigh-performance supercritical fluid chromatography – mass spectrometry for the qualitative analysis of metabolites covering a large polarity range. *J Chromatogr A*. 2022;1665:462832.
2. Gordillo R. Supercritical fluid chromatography hyphenated to mass spectrometry for metabolomics applications. *J Sep Sci*. 2021;44:448–63.
3. Losacco GL, Veuthey J-L, Guillarme D. Metamorphosis of supercritical fluid chromatography: a viable tool for the analysis of polar compounds? *Trends Anal Chem*. 2021;141:116304.
4. Lau JL, Dunn MK. Therapeutic peptides: historical perspectives, current development trends, and future directions. *Bioorg Med Chem*. 2018;26:2700–7.
5. Agrawal R, Belemkar S, Bonde C. Orthogonal separations in reversed-phase chromatography. *Chromatographia* 2018;81:565–73.
6. Shao Y, Wang C, Apedo A, McConnell O. Rapid separation of five cyclosporin analogs by supercritical fluid chromatography. *J Anal Sci Meth Instr*. 2016;06:23–32.
7. Zajickova Z, Nováková L, Svec F. Monolithic poly(styrene-co-divinylbenzene) columns for supercritical fluid chromatography–mass spectrometry analysis of polypeptide. *Anal Chem*. 2020;92:11525–9.
8. Enmark M, Glénne E, Leško M, Langborg Weinmann A, Leek T, Kaczmarek K, Klarqvist M, Samuelsson J, Fornstedt T. Investigation of robustness for supercritical fluid chromatography separation of peptides: isocratic vs gradient mode. *J Chromatogr A*. 2018;1568:177–87.
9. Zhang X, Scalf M, Westphall MS, Smith LM. Membrane protein separation and analysis by supercritical fluid chromatography–mass spectrometry. *Anal Chem*. 2008;80:2590–8.

10. Ventura M. Advantageous use of SFC for separation of crude therapeutic peptides and peptide libraries. *J Pharm Biomed Anal.* 2020;185:113227.
11. Tognarelli D, Tsukamoto A, Caldwell J, Caldwell W. Rapid peptide separation by supercritical fluid chromatography. *Bioanalysis* 2010;2:5–7.
12. Zheng J, Pinkston JD, Zoutendam PH, Taylor LT. Feasibility of supercritical fluid chromatography/mass spectrometry of polypeptides with up to 40-mers. *Anal Chem.* 2006;78:1535–45.
13. Blackwell JA, Stringham RW. Effect of mobile phase components on the separation of polypeptides using carbon dioxide-based mobile phases. *J High Resolut Chromatogr.* 1999;22:74–8.
14. Patel MA, Riley F, Ashraf-Khorassani M, Taylor LT. Supercritical fluid chromatographic resolution of water soluble isomeric carboxyl/amine terminated peptides facilitated via mobile phase water and ion pair formation. *J Chromatogr A.* 2012;1233:85–90.
15. Patel MA, Riley F, Wang J, Lovdahl M, Taylor LT. Packed column supercritical fluid chromatography of isomeric polypeptide pairs. *J Chromatogr A.* 2011;1218:2593–7.
16. Wang Y, Olesik SV. Enhanced-fluidity liquid chromatography–mass spectrometry for intact protein separation and characterization. *Anal Chem.* 2019;91:935–42.
17. Bennett R, Olesik SV. Protein separations using enhanced-fluidity liquid chromatography. *J Chromatogr A.* 2017;1523:257–64.
18. Molineau J, Hamel Y, Hideux M, Hennig P, Bertin S, Mauge F, Lesellier E, West C. Analysis of short-chain bioactive peptides by unified chromatography-electrospray ionization mass spectrometry. Part I. Method development. *J Chromatogr A.* 2021;1658:462631.
19. Molineau J, Hideux M, Hennig P, Bertin S, Mauge F, Lesellier E, West C. Analysis of short-chain bioactive peptides by unified chromatography-electrospray ionization mass spectrometry. Part II. Comparison to reversed-phase ultra-high performance liquid chromatography. *J Chromatogr A.* 2022;1663:462771.
20. Liu J, Regalado EL, Mergelsberg I, Welch CJ. Extending the range of supercritical fluid chromatography by use of water-rich modifiers. *Org Biomol Chem.* 2013;11:4925–9.
21. Liu J, Makarov AA, Bennett R, Haidar Ahmad IA, DaSilva J, Reibarkh M, Mangion I, Mann BF, Regalado EL. Chaotropic effects in sub/supercritical fluid chromatography via ammonium hydroxide in water-rich modifiers: enabling separation of peptides and highly polar pharmaceuticals at the preparative scale. *Anal Chem.* 2019;91:13907–15.
22. Spelling V, Stefansson M. Evaluation of chromatographic parameters in supercritical fluid chromatography of amino acids as model polar analytes and extended to polypeptide separations. *J Chromatogr A.* 2020;1633:461646.
23. Govender K, Naicker T, Baijnath S, Chaturgoon AA, Abdul NS, Docrat T, Kruger HG, Govender T. Sub/supercritical fluid chromatography employing water-rich modifier enables the purification of biosynthesized human insulin. *J Chromatogr B.* 2020;1155:122126.
24. Losacco GL, DaSilva JO, Liu J, Regalado EL, Veuthey J-L, Guillaume D. Expanding the range of sub/supercritical fluid chromatography: advantageous use of methanesulfonic acid in water-rich modifiers for peptide analysis. *J Chromatogr A.* 2021;1642:462048.
25. Govender K, Naicker T, Baijnath S, Kruger HG, Govender T. The development of a sub/supercritical fluid chromatography based purification method for peptides. *J Pharm Biomed Anal.* 2020;190:113539.
26. Vosloo JA, Rautenbach M. Following tyrothricin peptide production by *Brevibacillus parabrevis* with electrospray mass spectrometry. *Biochimie.* 2020;179:101–12.
27. Tang X-J, Thibault P, Boyd RK. Characterisation of the tyrocidine and gramicidin fractions of the tyrothricin complex from *Bacillus brevis* using liquid chromatography and mass spectrometry. *Int J Mass Spectrom Ion Processes.* 1992;122:153–79.
28. D'Hondt M, Gevaert B, Wynendaele E, De Spiegeleer B. Implementation of a single quad MS detector in routine QC analysis of peptide drugs. *J Pharm Anal.* 2016;6:24–31.
29. Eugster PJ, Biass D, Guillaume D, Favreau P, Stöcklin R, Wolfender J-L. Peak capacity optimisation for high resolution peptide profiling in complex mixtures by liquid chromatography coupled to time-of-flight mass spectrometry: application to the *Conus* consors cone snail venom. *J Chromatogr A.* 2012;1259:187–99.
30. Neue UD. Theory of peak capacity in gradient elution. *J Chromatogr A.* 2005;1079:153–61.
31. Gilar M, Daly AE, Kele M, Neue UD, Gebler JC. Implications of column peak capacity on the separation of complex peptide mixtures in single- and two-dimensional high-performance liquid chromatography. *J Chromatogr A.* 2004;1061:183–92.
32. Wren SAC. Peak capacity in gradient ultra performance liquid chromatography (UPLC). *J Pharm Biomed Anal.* 2005;38:337–43.
33. Meek JL, Rossetti ZL. Factors affecting retention and resolution of peptides in high-performance liquid chromatography. *J Chromatogr A.* 1981;211:15–28.
34. Brown PR. Effect of flow rates and the slope of the linear concentration gradient on peak areas in high pressure liquid chromatography. *J Chromatogr A.* 1971;57:383–90.
35. Tarafder A. Designs and methods for interfacing SFC with MS. *J Chromatogr B.* 2018;1091:1–13.

**How to cite this article:** Neumann J, Schmidtsdorff S, Schmidt AH, Parr MK. Application of sub-/supercritical fluid chromatography for the fingerprinting of a complex therapeutic peptide. *J Sep Sci.* 2022;45:3095–3104. <https://doi.org/10.1002/jssc.202200393>